The Unknown of the Pandemic: An Agent-based Model of Final Phase Risks

Marco Cremonini* Samira Maghool†

April 24, 2020

Abstract

With the COVID-19 pandemic progressing after the peak, public health authorities are facing the difficult decision of how to manage the final phase of the epidemic wave. Diffuse uncertainty still persists about the characteristics of the pandemic and its actual dynamics, in particular with regard to the real extent of undiagnosed infected cases. We present a discrete-time stochastic model with state-dependent transmission probabilities and multi-agent simulations focusing on possible risks that could materialize in the final phase of the epidemic. The results of our experiments show that, in different scenarios, there is the possibility that unknown undiagnosed cases still looms when diagnosed infected cases are close to be extinguished. We study variants of base scenarios to account for uncertain epidemiological estimates and the effects of testing and containment of cases otherwise undiagnosed. A trade-off between measures producing a slower or accelerated dynamics is discussed. Ultimately, the analysis we have presented highlights that the enduring uncertainty, characterizing the current pandemic, calls for risk analyses approaches to complement epidemiology studies.

1 Introduction

Uncertain estimates on the proportion of undetected COVID-19 cases have been repeatedly suggested, with epidemiologists raising the alarm that covert cases, mostly asymptomatic or mildly ill, are likely to be the driving factor of the epidemic's dynamics [35, 16]. In many countries, the attention is now turning to the final phase of the epidemic wave [10], which likewise could present unforeseen and, in some scenarios, severe risks caused by undetected cases [34, 30]. The critical situation that could arise is that when diagnosed cases will considerably reduce and the pressure on national health systems will be relieved, the risk of a

*Department of Social and Political Science, University of Milan, Italy.
email: marco.cremonini@unimi.it
†Computer Science Department, University of Milan, Italy.
email: samira.maghool@unimi.it

new rebound in transmission caused by the looming presence of undetected infectious cases could be difficult to assess for public health authorities. Strategies for reopening activities and lifting restrictions will likely be under the pressure of the predominant individualistic approach to pandemic risks [11], with decision based on risk assessment processes heavily influenced by the uncertainty still characterizing the COVID-19 dynamics [12].

Our research goal is to analyze the possible consequences of uncertain estimates of undetected infectious cases in a risk analysis perspective and the natural dynamics of the network under several scenarios. To this end, by considering available evidences from epidemiological and virologist studies, we focus on a specific *research question*: Under which conditions, as a result of the natural evolution of the model, in the final phase of an epidemic wave the undetected infectious cases could represent a high risk situation? In particular, we deem a situation as *high risk* if: *i)* undetected infectious cases cannot be safely approximated by officially diagnosed cases; *ii)* different scenarios and their variants exhibit relevant and variable differences between the dynamics of undetected infected cases and of those officially recorded.

Apparently, this is a question still unanswered by current analyses of 'exit strategies' from lockdown and other mitigation measures. For example, even [12], which are publishing truly excellent reports on the France situation and have presented a rich model and a detailed analysis of possible strategies for the final phase of the epidemic wave, have not addressed that question. Rather, they concentrated on more specifically epidemiological issues, like the possible overwhelming of medical facilities due to a rebound of the epidemic. Coherently, they observed that exit strategies would be more effective the larger the proportion of infected cases not requiring hospitalization, such as asymptomatic and mildly ill cases.

While their analysis and others in the same vein are meaningful and informative for public health decisions, they do not really tackle with the problem of deciding under what conditions of the epidemic dynamics, considering the persistent uncertainty about the characteristics of the contagion, the epidemic could be safely declared under control. Our aim is to contribute to identify some properties of the system dynamics that are relevant in the final phase of the epidemic wave. By developing a compartmental multi-agent model, we have observed interesting behaviors of the class of undetected infectious cases, which, depending on the scenario, could be not under control when, instead, observed diagnosed cases seem to indicate a safe situation. Modeling possible dynamics of the contagion with variable configurations of undetected infectious cases could be useful for a better comprehension of the consequences of the uncertainty still looming and given the still enduring difficulty in testing or tracing undiagnosed infectious cases. Major findings of our work are that:

- risk situations due to undetected asymptomatic or mildly ill cases may arise if they largely outnumber fully symptomatic cases;
- the larger the proportion of undetected cases with respect to fully symptomatic ones, the less suitable is the number of detected diagnosed cases

(i.e., contained in hospital facilities or home isolated) as an approximation of the uncertain undetected cases;

- the more asymptomatic or mildly ill cases are diagnosed and contained along the whole epidemic wave, the safer is the situation in the final phase of the epidemic wave.

In this work, we use a compartmental model, as for long tradition of studies combining epidemiological theory and network theory [23, 32]. We study three hypothetical scenarios for the final phase of the epidemic wave, with 10%, 30%, and 50% of total infected individuals, diagnosed and undiagnosed, with respect to the reference population (infection attack rate). The range of variability of these scenarios is wide, with the largest case envisioning an extreme outcome, which, for what we currently know, cannot be deemed as completely unrealistic, according to actual guesses of some epidemiologists [2, 33, 4], from journalistic reports [6, 25, 1], and from estimates made for the 2005 avian H5N1 infection [15]. For each scenario, we have varied the proportion of undetected and detected cases, ranging from a minority of undetected cases, as typical for the 2002-2003 SARS [3], to a majority of undetected cases, as now conjectured. Variants and special cases have been considered.

The rest of the paper is structured as follows. First, we introduce the compartmental model by presenting the state transition diagram with a description of compartments. Then, we describe the model execution with the initialization of parameters and fitting with respect to data from Italian and World outbreaks. Next, we present simulation results starting with the first scenario (i.e., 30% Scenario) and varying proportions of undetected and detected cases, followed by the other two (i.e., 10% and 50% Scenario). Then, we consider variants by changing some of the initial assumptions, related to the viral load between compartments and the possible transmission from contained state, and perform a sensitivity analysis on the infectious period while incubating the disease, a parameter that has received different estimates from epidemiological studies. After that, we discuss the effects on the uncertainty in the final phase of the epidemic wave of an increasing proportion of asymptomatic and mildly ill cases diagnosed and contained. Finally, we discuss the results and draw some conclusions.

2 Model Definition

We present a discrete-time stochastic model with state-dependent transmission probabilities derived from others developed to study pandemic influenza [15, 28, 29], the SARS dynamics of 2002-2003 [7], and the current SARS-CoV-2 pandemic [27]. Individuals when infected proceed through different stages (biological or due to isolation constraints), with varying transmission probabilities. For example, an individual first incubates the infection, then s/he might develop full symptoms, and then is diagnosed and isolated. These three states have different transmission probabilities in the model. Analogously, another individual could incubate the infection and develop only mild symptoms, possibly

misinterpreted as a normal cold, and for this reason neither be diagnosed nor isolated until the spontaneous recovery. In this case, s/he only goes through two infectious states in the model, with different transmission probabilities. In addition to state-dependent transmission probabilities, our model also accounts for different probability distributions of the time spent in a state, such as the time spent incubating the infection, the time with full symptoms before being diagnosed and isolated, or the time spent freely roaming the contact network being infected but with mild symptoms before the spontaneous recovery.

2.1 State Transition Diagram

The definition of our model's compartments and state transition diagram inherits intuitions from the literature and adds some variations to better serve to our research goal [14, 37, 20, 36]. In Figure 1, we show the state transition diagram with compartments as nodes and edges labeled with transition probabilities. For sake of clarity, transition probabilities are showed with a notation different from typical epidemiological studies, which adopt Greek letters. Here a probability is showed with a single parameter when meant to be the probability to remain in current state (e.g., P(S) is the probability of an agent to remain susceptible); instead, it is showed with two parameters to denote the probability to change state (e.g., P(II,AI) is the probability of an incubating infected node (II) to move in the acute infected state (AI)). For all transitions except one, the diagram is a discrete-time memoryless Markov chain. The exception is the state transition from Contained (C) to Recovered (R), which depends on the previous transition, because from epidemiological studies and medical reports of the COVID-19 pandemics [27], the probability distribution of the recovery time has clearly distinct ranges for individual with mild or acute infection. Choosing a single state C has been done to keep the model as simple as possible, the trivial solution would have been with two distinct C states, for Mild and Acute individuals, with no advantage for our study. Table 1 summarizes the

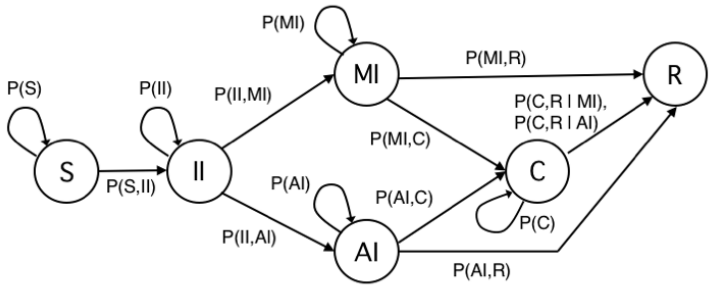

Figure 1: State transition diagram consisting of six states: S (Susceptible), II (Incubating Infected), MI (Mild Infected), AI (Acute Infected), C (Contained), and R (Recovered/Removed).

characteristics of compartments.

Table 1: Model's compartments with description of characteristics and assumptions for simulations.

Symbol	Compartment	Description
S	Susceptible	The initial state for all individuals in the model except the ones seeding the epidemic. At each discrete time step, individuals interact through the contact network with directly connected peers and could become infected with a certain probability that depends on the number of infected peers and their infected state (II, MI, AI, or, but only for some simulations, C).
II	Incubating Infected	Incubating infected are Susceptible individuals that become infected. Infectivity develops in this phase, although reduced with respect to the symptomatic state, according to current medical analyses. This is the state assigned to the initial seeding nodes in simulations. Individuals stay in this state according to a probability distribution within a time frame derived from the literature.
MI	Mild Infected	Infected persons showing no symptoms or mild symptoms easily misdiagnosed or, due to the mildness of the condition, reluctant to self-quarantine and look for medical assistance. Persons in this state are often assumed to carry a reduced viral dose with respect to those that develop full acute symptoms. MI individuals could at some point be diagnosed and contained (state C) or they remain in the same state until spontaneous recovery (state R). A special case has also been tested for the hypothesis of MI cases carrying a full viral dose.
AI	Acute Infected	Infected persons that develop full symptoms and carry the full viral dose. We assume that all AIs certainly receive a diagnose within a time frame, and then move to state C. The possibility that AI individuals are not diagnosed and thus contained exists in practice and the state diagram shows the corresponding probability. However, in simulations, we have considered that case as not relevant for the outcome and ignored.
C	Contained	Infected persons that have been diagnosed and then isolated. Our base assumption is that individuals in state C do not transmit the infection to peers and move to recovery/removed (state R) according to a probability distribution within a time frame derived from the literature. The time frame is different for the case of an individual in C being previously AI or MI. The possibility of contained infected individuals spreading the disease is of course very well-known (e.g., in hospitals or other medical facilities). We have considered this case and run some simulations with different probability of transmission also from C individuals.
R	Recovered/Removed	This is the final state of the transition diagram reached by all individuals in our model. The transition from MI or from C depends on probability distributions within different time ranges.

With regard to the model's state transition diagram, we add here some context and details to the definitions given in Table 1. The Incubating Infected (II) state has a specific characterization in our model, different from the typical definition. A state representing the disease incubation time has a long tradition in deterministic and stochastic models in epidemiology [20]. Among compartmental models, the standard SEIR dubbed it Exposed [8], which became Latent in other SLIAR models, specifically referring to incubating but not infectious persons [27, 5]. Others, like [19], studying the 2002-2003 SARS epidemic, did

not consider a specific state for those incubating the disease being not infectious. Instead, they defined an Asymptomatic compartment as the first stage for all susceptible cases turned infected. In that state, persons are infectious and could possibly be quarantined or develop a fully symptomatic state. With respect to our research goal, these approaches are not suitable for our goals. There is no purpose in our model to specify an incubating not infectious state, because irrelevant for the study of the dynamics of infectious individuals being isolated or free to roam their contact network. On the other hand, regarding the current COVID-19 epidemic, different epidemiological studies analyzing samples from China and Singapore outbreaks have reached the conclusion that individuals could develop infectivity in the incubation period [26, 17]. Being this possibility relevant for our study, we have included the Incubating Infectious (II) state with the specific meaning of modeling the time period of infectivity during the disease incubation. The probability distribution of the time spent in this state has been obtained from [27].

The distinction between symptomatic and asymptomatic infected individuals was originally introduced by [28] as an extension of the standard SEIR model, by postulating the fundamental assumption that only the symptomatic cases withdraw with some probability to a restricted place (e.g., home confined, hospitalized). Most recent epidemic models, conveniently customized, are based on that distinction [8]. Following the introduction of the two classes for the symptomatic and the asymptomatic cases, models have attempted to manage the different social impacts. In [8], the two new classes are added to represent different forms of social distancing: Generic quarantine for the asymptomatic and specific isolation for the symptomatic. The quarantine compartment is useful for modeling the dynamic of the contagion when a social distancing policy is enforced by the public health authority (e.g., national/federal state, regional/local authority) in order to limit contacts between casual susceptible persons and undiagnosed infected individuals, untested and often asymptomatic [12]. Differently, symptomatic infected are supposed to be diagnosed and strictly isolated, for example in a medical facility or hospital, within a certain time frame from the outset of symptoms or after a positive test. With respect to our goal, we have considered the quarantine state as not strictly needed. What matter most to us is to account for the ability to spread the contagion of all undiagnosed infected individuals, according to a certain transmission probability that we estimate to determine a given attack rate (i.e., our 10%, 30%, and 50% scenarios). To this end, we do not distinguish if the final attack rate has been produced by reducing contacts (as for isolation measures like generalized quarantine) or because of a reduced infectivity; in both cases the final attack rate is the same. Consequently, in our model, we have included only two states called Mild Infected (MI) and Acute Infected (AI). Next, we added a single Contained (C) state for all individuals infected, diagnosed, and restricted. For our research goal, the Contained compartment serves the purpose of modeling those whose ability to spread is greatly reduced by means of personal containment measures, with respect to others without limitations (or only subject to a general social distancing policy). With regard to the infectious states, we make the hypoth-

esis that information networks, the press, and generic public opinion makers, in the final phases of the epidemic wave, will be primarily influenced by the dynamics of the Acute Infected and the Contained classes, as recorded by official statistics, with risks brought by the mostly unknown Mild Infected class not well acknowledged. The emphasis over observable AI and C states and the uncertainty regarding the mostly speculative MI state would put public health authorities under pressure for immediate lift of isolation measures based on the dynamics of the former two states, and instead would assess with great difficulty the behavior of the third one.

The last compartment of our model is the traditional Recovered/Removed (R), which accounts for all individuals that end the epidemic process and have acquired immunization or deceased. In this work, we do not consider the case of re-infection and temporary immunization. One reason is because we explicitly aim to focus on the last period of the first epidemic wave and the potential risks due to undiagnosed infected, therefore we assume that even in case of temporary immunization, the rate of re-infections would be not particularly relevant in that time frame. Another reason is that at present, to the best of our knowledge, the possible temporary immunization for COVID-19 patients is still a hypothesis investigated by medical researchers and epidemiologists.

3 Model Execution

The model is run through multi-agent simulations [9, 22] and makes use of an artificial random network representing contacts. The basic execution of the model is described in Algorithm 1. Each iteration represents a time step in simulation time. At every time step, each node is selected in random order and, if in state S its state is checked with respect to peers, or if in other states, according to time periods specific of states II, MI, AI, and C. The probability of a node S to become infected depends on infected peers II, MI and AI, independently (μ is the reduction factor to account for possibly reduced viral dose of II and MI).

3.0.1 Initialization and Parameters Fitting

Figure 2 describes the model initialization with actual transitions and probabilities. Table 2 presents a description of transition probabilities and of their values. The list of base settings for simulations is in Table 3.

Infection propagation is modeled starting with a general transmission probability empirically evaluated with respect to each one of reference scenarios (i.e., 10%, 30%, or 50% infection attack rate). This general transmission probability represents the infectivity of a full viral dose, which is present in individuals developing acute symptoms (AI compartment). The transmission probability is reduced for individuals in different conditions, namely incubating the infection and with mild symptoms.

We first found the settings for the 10%, 30%, and 50% scenarios. The population considered for simulation results was N=1000 (we also run sample simu-

Algorithm 1 Time-discrete multi-agent model execution

Require: Adjacency matrix ($A_{i,j}$), selecting random seeds, attributing the T_{II} , T_{MI} , T_{AI} , $T_{C|MI}$ and $T_{C|AI}$ to each nodes according to defined distributions

for t in Timesteps **do**
for i in $A_{i,j}$ **do**
At each time step t, for all nodes in $A_{i,j}$, run the model according to the current node's state
Case S:
if $Node_i$ in state S **then**
for j in $A_{i,j} = 1$ **do**
if $Node_j$ in state AI **then**
Change state to II with probability P(S,II)
end if
if $Node_j$ in state (II,MI) **then**
Change state to II with probability μP(S,II)
end if
end for
end if
Case II:
if $Node_i$ in state II **then**
Remain in II for $T_{II}(i) = gamma(\alpha_1, mean_1/\alpha_1)$ steps
if $rand[0,1)] < MI/(MI + AI)$ **then**
Change state to MI
else
Change state to AI
end if
end if
Case MI:
if $Node_i$ in state MI **then**
Remain in MI for $T_{MI}(i) = norm(T_{MI})$ steps
When $T_{MI}(i)$ expires:
if $rand[0,1)] < P(MI, C)$ **then**
Change state to C
else
Change state to R
end if
end if
Case AI:
if $Node_i$ in state AI **then**
Remain in AI for $T_{AI}(i) = gamma(\alpha_2, mean_2/\alpha_2)$ steps
When $T_{MI}(i)$ expires, change state to C
end if
Case C:
if $Node_i$ in state C **then**
if $Node_i(t-1)$ changed state from MI **then**
Remain in C for $T_{C|MI}(i) = norm(T_{C|MI})$ steps
else if $Node_i(t-1)$ changed state from AI **then**
Remain in C for $T_{C|AI}(i) = norm(T_{C|AI})$ steps
end if
end if
Case R:
if $Node_i$ in state R **then**
Remain in R
end if
end for
end for

Table 2: State transition probabilities and values used in simulations.

Probability	Description	Values
P(S)	p. to remain susceptible. It is fitted empirically according to the scenario considered, 10/30/50% total infected resulting at the end of the epidemic with respect to the whole population. $P(S) = 1 - P(S, II)$.	0.99 (10% scenario); 0.98 (30% scenario); 0.97 (50% scenario).
P(S,II)	p. to get infected (transmission rate). Empirically evaluated. $P(S, II) = 1 - P(S)$.	0.01 (10% scenario); 0.02 (30% scenario); 0.03 (50% scenario)
P(II)	p. to remain in incubation state. The probability is defined as the probability distribution over the time range T_{II}.	For each node $gamma(T_{II})$, with T_{II} in [2,14], as estimated in (19), with k = 3 and mean = 8.
P(II,MI)	p. to move from the incubation state II to the MI state. This is the main unknown of the study.	Simulations have been run with different values for the pair MI:AI=(0.8:0.2, 0.6:0.4, 0.4:0.6, 0.2:0.8).
P(II,AI)	p. to move from the incubation state II to the AI state.	See P(II,MI) values.
P(MI)	p. to remain in state MI. The probability is defined as the probability distribution over the time range T_{MI}.	For each node, $norm(T_{MI})$, with T_{MI} in [2,7], as estimated in (19).
P(MI,C)	p. to move from MI to C. It measures the odds of an MI individual to be diagnosed and thus isolated.	The worst case scenario is to consider P(MI,C)=0, meaning no MI is detected and isolated. We also considered other values, i.e., 0.2, 0.5 and 0.8, to account for increasing proportions of MI being detected and contained.
P(MI,R)	p. to recover for a MI individual. The probability depends to P(MI) and P(MI,C).	When T_{MI} steps expire, the node in MI move to R (unless previously moved to C). $P(MI, R) = 1 - (P(MI) + P(MI, C))$.
P(AI)	p. to remain in state AI before being moving to C. The probability is defined as the probability distribution over the time range T_{AI}.	For each node, $norm(T_{AI})$, with T_{MI} in [2,7], as estimated in (19).
P(AI,C)	p. to move from AI state to C. It depends only on the value of P(AI).	When T_{AI} steps expire, the node in AI move to C. $P(AI, C) = 1 - P(AI)$
P(AI,R)	p. to recover for an MI individual without being diagnosed and contained. We assume this case as non-existent.	$P(AI, R) = 0$.
P(C)	p. to remain in C state. The evaluation of this probability is different for nodes arrived in state C from MI or from AI, being the time intervals completely distinct for the two cases. The probability then is defined as the probability distribution over two time ranges $T_{C\|MI}$ and $T_{C\|AI}$.	For each node, $norm(T_{C\|MI})$, with $T_{C\|MI}$ in [2,5] if the node was previously in state MI, or $norm(T_{C\|AI})$, with $T_{C\|AI}$ in [14,30] if the node was previously in state AI. The time ranges are defined from medical reports and (19).
P(C—MI,R)	p. to recover from C state being MI. It depends on the value of P(C) evaluated with respect to $T_{C\|MI}$.	For each node, when $T_{C\|MI}$ steps expire, the state changes from C to R.
P(C—AI,R)	p. to recover from C state being AI. It depends on the value of P(C) evaluated with respect to $T_{C\|AI}$.	For each node, when $T_{C\|AI}$ steps expire, the state changes from C to R.
P(R)	p. to stay in R state, our final state.	$P(R) = 1.0$.

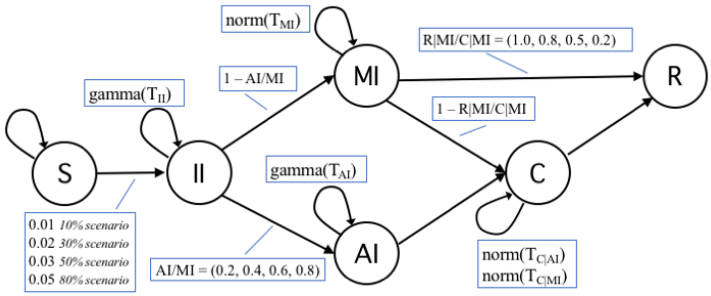

Text boxes represent the settings of the corresponding transitions. In some cases, they are indicated as a probability distribution over a time period (e.g., $gamma(T_{II})$), as lists of alternative values that have been tested (e.g., 0.01, 0.02, and 0.03 for the transmission probability of Susceptible individuals), or as complements (e.g., 1-R—MI/C—MI, meaning the corresponding list 0.0, 0.2, 0.5, 0.8). For simplicity, for state S, and edges AI-C and C-R, the value has been omitted, because only two outgoing edges are present.

Figure 2: Model initialization.

Table 3: Base simulation settings.

Parameter	Values
Network size	1000
Seed nodes	5
Time steps	150
Probability of transmission (full viral dose)	0.01 (10% Scenario), 0.02 (30% Scenario), 0.03 (50% Scenario)
Reduction factor (reduced viral dose)	$\mu = 0.5$
Latency time	time steps=[2,14], mean=8
Infectious time - Acute Infected	time steps=[2,7], mean=3
Infectious time - Mild Infected	time steps=[2,7], mean=4.5
Isolation period - Acute Infected	time steps=[14,30], mean=22
Isolation period - Mild Infected	time steps=[2,5], mean=3.5
Acute Infected : Mild Infected	0.2, 0.4, 0.6, 0.8
Mild Infected Contained : Not Contained	0.0, 0.2, 0.5, 0.8

lations with N=10000 and N=100000 and found that results were qualitatively similar). Empirically, we found that the best fitting values for the transmission probability (i.e., P(S,II) in the state transition diagram) were (0.01, 0.02, 0.03) respectively for the three scenarios. Seed nodes used in simulations have been five, a number representing a good trade-off in order to reduce the number of invalid trials without relevant effects to the average number of infected nodes. A trial was considered invalid, thus discarded, if it produced less than 1/5 of infected nodes with respect to the average proportion defined for the specific scenario, and we considered the settings sufficiently accurate when the average total number of infected nodes calculated over all valid trials was $\pm 3\%$ of the proportion (attack rate) required by the scenario. For states II and AI, we adopted a time-to-event observation model with a gamma distribution of the time T_{II} and T_{AI} an individual remains in each of those states. For states MI and C, instead, we assumed a normal distribution of time T_{MI} and T_C. Parameters for gamma and normal distributions, as well as of the lengths of these periods of time have been derived from [27] (in a different study [31], both the probability distribution and the incubation period have received a different estimation, we took [27] as our reference study being based on a larger sample). In all figures, each data point was averaged over at least 150 valid trials. Table 3 summarizes the parameters and settings for simulations.

Model configurations have been studied to fit publicly available data of Italian cases (national time series, Lombardy region, Bergamo and Lodi provinces) and World cases (New York City and national time series of China, Iran, and Spain). As a result, we found that the 10%, 30%, and 50% scenarios, with adaptations hereafter discussed, are well-suited to provide an approximate, while realistic, representation of the epidemic growth rates. Details about specific time periods and model fitting are presented in Figure 3.

4 Results

4.1 30% Scenarios

In the first group of simulations, for each scenario we compared the network behavior with a majority of MI individuals with respect to the opposite case of a larger proportion of AI individuals. With these simulations, our aim is to show how a large proportion of MIs may produce a distinct behavior during the epidemic with respect to the opposite case. In particular, this specific behavior may result in a risk scenario during the final phase of the epidemic. We show how the effect changes with different proportions of AI and MI.

First, we analyze results for the 30% Scenario (see Figure 4), which sits between the lower 10% Scenario, perhaps an estimate that some countries are already approaching, with the epidemic still far from being terminated, and the 50% Scenario. Results shows that in all cases with MI larger than AI, in the final phase of the epidemic, there is a substantial difference between the density of MI and of AI. By assuming the same criteria of [29] to consider an

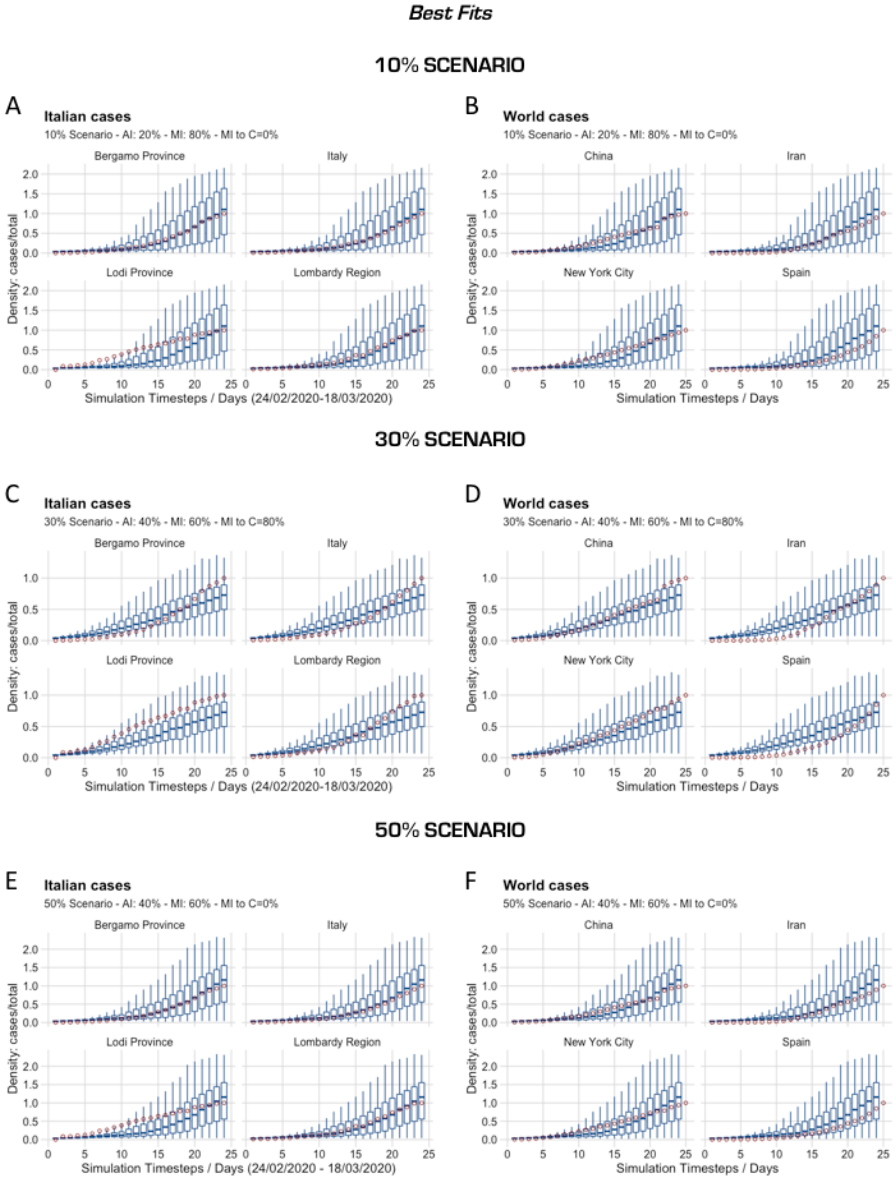

Italian cases: Days: 24/02-18/03/2020; Source: Civil Protection Department [13]. *World cases*: China - Days: 22/01-15/02/2020; Source: The Humanitarian Data Exchange (HDE) [38]. Iran - Days: 20/02-15/03/2020; Source: HDE. New York City - Days: 15/03-08/04/2020; Source: The New York Times [39]. Spain - Days: 03/03-28/03/2020; Source: HDE.

Figure 3: Best fitting configurations with respect to Italian and World cases.

epidemic as contained if there are fewer than 500 cases in the 500,000-person community (¡1 per 1000), the difference between AI and MI could surpass one order of magnitude, with the larger difference corresponding to more unequal proportions between AI and MI (i.e. in Figure 4 panels A, B, and C, the AI curve reaches the threshold of 1/1000 at approximately the 110 intercept on the x-axis). It is not until the end of the duration of the simulation that the MI reaches the threshold of 1/1000. In practical terms, we could probably assume that the difference between AI and MI behavior could correspond to a period of some weeks, during which, based on official statistics of diagnosed infected, the epidemic would be mistakenly considered as contained. This is the risky situation that we want to highlight with this work. On the contrary, the dynamics of AI and MI is equivalent or with AI terminating later than MI, for cases with a majority of AI (i.e. Figure 4 panels D and E). From a risk analysis perspective, the case of the previous SARS epidemic with few asymptomatic cases, is structurally different from the mostly accepted hypothesis regarding the current one. The possibility of unaccounted dangerous conditions for the insurgence of a novel uncontained outbreak did not naturally arise during the 2002-2003 SARS but, instead, there is this possibility for COVID-19. Clearly, this observation regards the natural dynamic behavior, as modeled here. It does not consider the effectiveness of public health authorities decisions. For these tests, we have worked under the assumption that MI individuals have a viral load reduced by approximately 50% with respect to AI, as reported in past and recent studies [29, 27]. Correspondingly, the probability for a Susceptible individual to get infected when in contact with a MI person has been reduced in our model (Reduction factor in Table 3). However, this assumption seems still debated in the literature. In [40], the viral load between symptomatic and asymptomatic infected persons has been measured as similar.

4.2 Other Scenarios

Figure 5 and Figure 6 present the 10% Scenario and the 50% Scenario, which, together with the 30% Scenario discussed in Figure 4, complete the overview of the studied scenarios. These two additional cases qualitatively confirm what already discussed for the 30% Scenario:

- the risk scenario due to the unknown rate of MI might arise for MI larger than AI;
- the larger the proportion of MI with respect to AI, the less suitable is C as an approximation of MI.

With respect to the different prevalence among scenarios, what could be observed is that the larger prevalence (i.e. 50% Scenario) produces a higher number of infected, but on the other side, the dynamics naturally tends to accelerate with a shortened average time to extinction of all compartments. The accelerated behavior is reflected in the higher density of the R class that accompanies the corresponding higher density of infected II, AI, and MI classes.

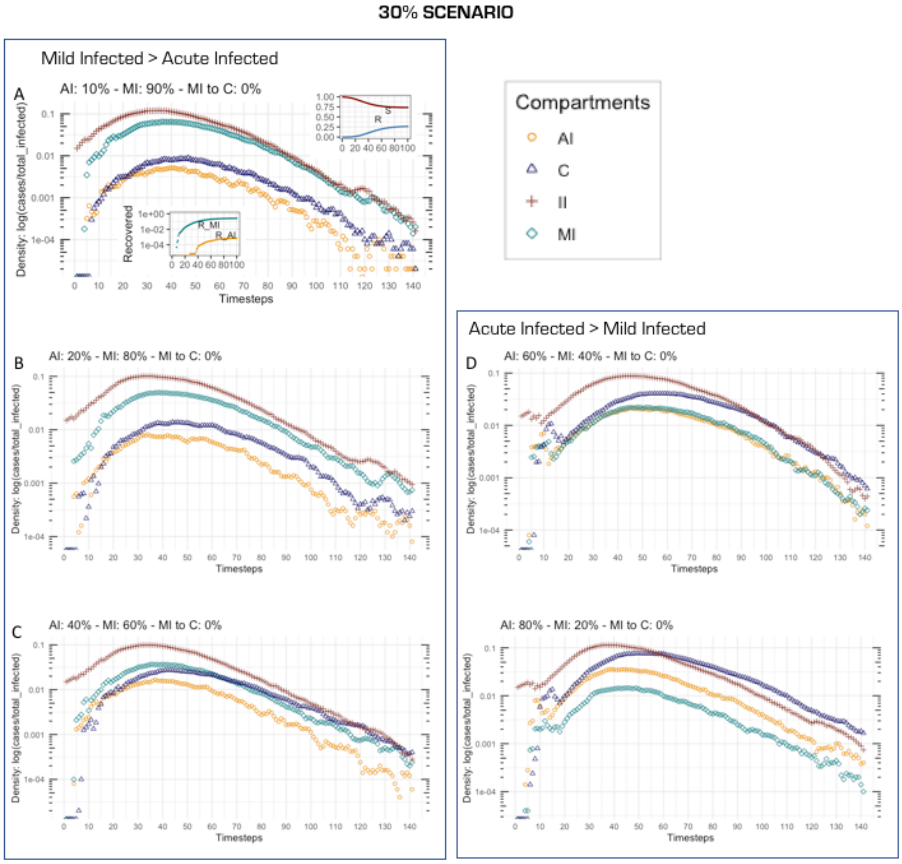

Each data point has been averaged over 150 trials. *Panels A, B, and C*: Results for configuration with a proportion of MI greater than AI (i.e., respectively for A, B, and C, AI:MI = 10:90, 20:80, 40:60). *Panels D and E*: Cases with the proportion of AI greater than MI (i.e., AI:MI = 60:40, 80:20 for E and D). *Panel A, top-right inset*: The aggregate dynamics of compartment R and S. *Panel A, bottom-left inset*: Detailed representation of compartment R's dynamic separated into the subgroup of those recovering from MI (R_{MI}), and those recovering from AI (R_{AI}).

Figure 4: 30% Scenario, results for different proportions of AI:MI.

The aggregate dynamics of R in the different scenarios could be observed in the top-right inset of panel A of Figure 5 and Figure 6. In the bottom-left inset of panel A, instead, it could be observed the details of the dynamics of compartment R, separated into those recovering from MI (R_{MI}), and those recovering from AI (R_{AI}). Again, the MI compartment dominates the overall system dynamics. We remark the fact that the acceleration of the dynamics represents a natural tendency of the system, it does not consider the practical consequences of a steeper and larger increase of infected, which could easily produce cascade effects on the emergency facilities and medical infrastructures, or the introduction of stricter social distancing measures.

4.3 Special Cases

4.3.1 No Viral Load Reduction for Incubating and Mild Infected

In this first special case, we consider the hypothesis that there is no reduction of the viral load for incubating and mild infected cases with respect to individuals developing full symptoms, as measured in [40]. Figure 7 shows the results of simulations with this variant for the 30% Scenario (Reduction factor $\mu = 1.0$). The effect is mixed and reveals a particular behavior that naturally arises in another case too, and could be counterintuitive. With a higher transmission probability of the MI class, the total number of infected increases, as well as the proportion of MIs.

The combination of the two seemingly lead to worsening all aspects of the epidemic. However, also the overall dynamics accelerates. Figure 7 shows the comparison between the variant with equal transmission probability (color) and the original results from Figure 4 (grey). What emerges as a general property, is that the accelerated behavior, in theory, makes the risk of the final phase less severe, because all compartments tend to decade faster and closer in time. This is a representation of the theoretical benefit of a faster, unmitigated epidemic, with respect to a delayed slower dynamics. In practice, that theoretical benefit clashes with at least two fundamental factors of epidemic containment. First, the practical, possibly tragic effects of an uncontrolled epidemic on hospital facilities, medical supplies, and the capability of the emergency response process to deal with the epidemic. Secondly, a slower dynamics permit to gain time to learn to public health authorities and to test unknown characteristics of the epidemic. However, it should be helpful to have a clear representation of the fact that a slower epidemic dynamics is not necessarily better than a faster one. With regard to other scenarios, they confirm the possible presence of the risk due to undetected MIs in the final phase of the epidemics, proportionally larger the more MIs are present in the population. It also confirms the changes on the dynamics due to an increasing number of infected, with the 50% Scenario faster than 10% and 30% scenarios, and thus less prone to the risk posed by MIs.

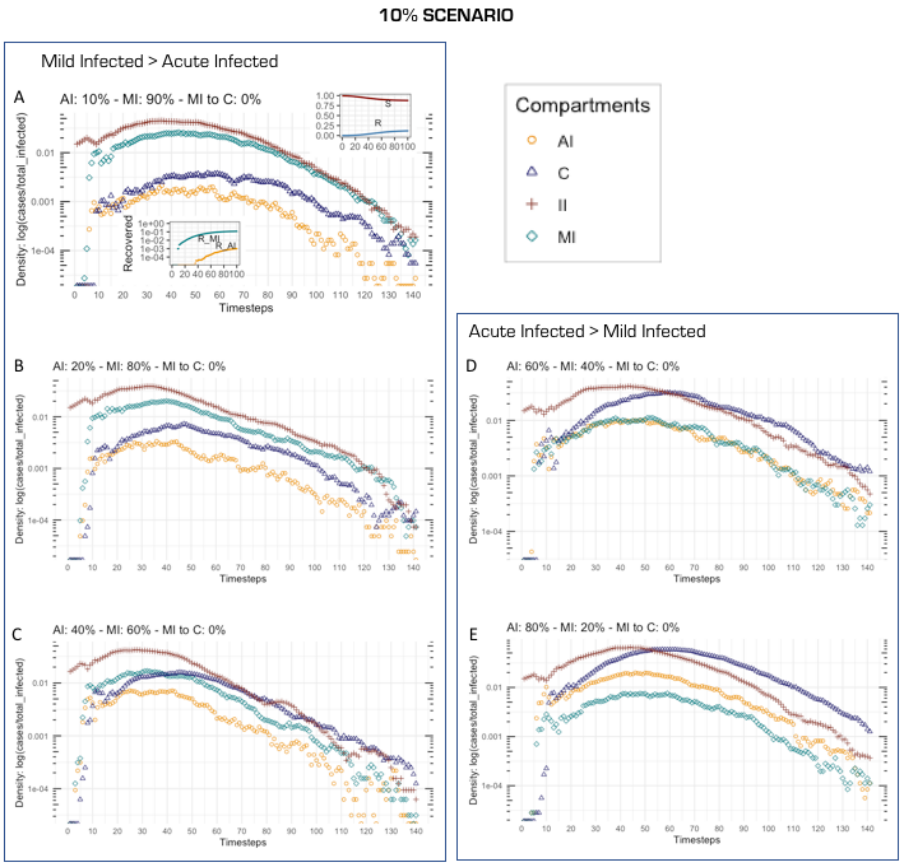

Figure 5: 10% Scenario, results for different proportions of AI:MI.

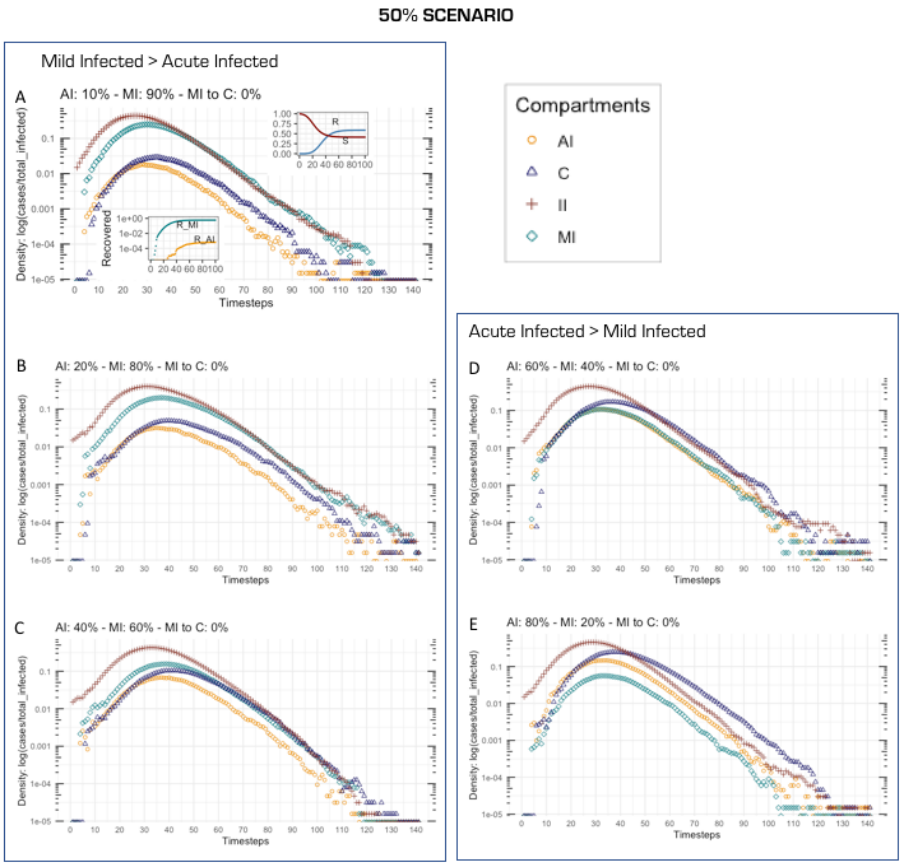

Figure 6: 50% Scenario, results for different proportions of AI:MI.

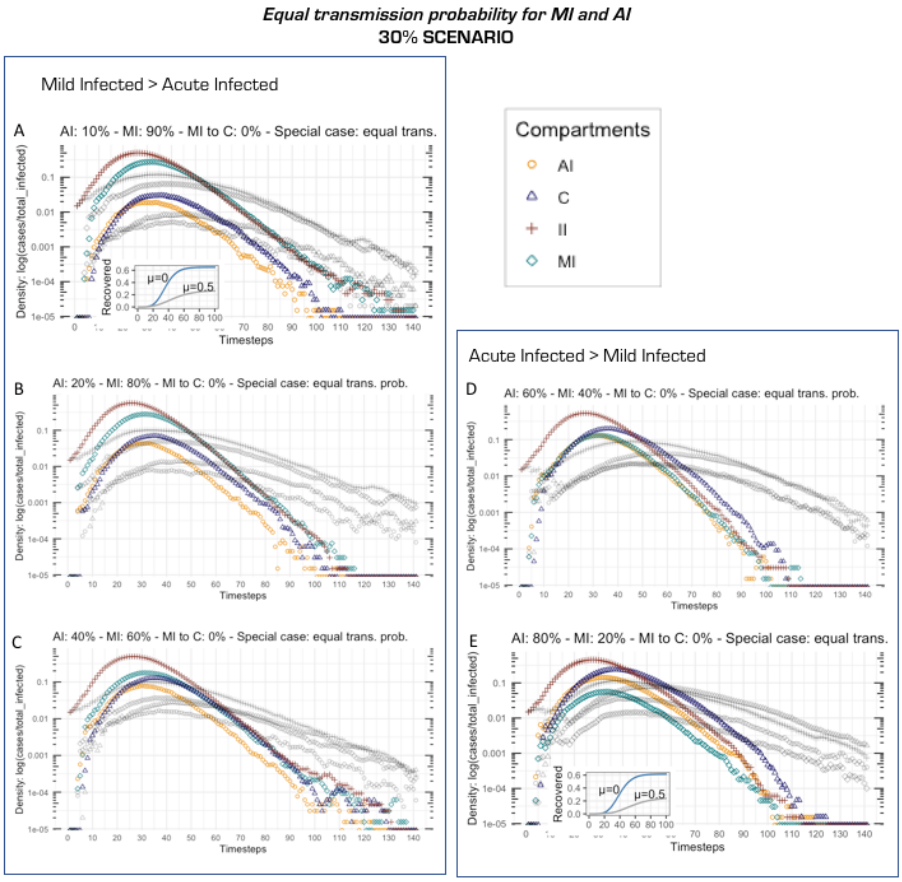

Each panel presents a comparison between the case with equal transmission probability for II, MI, and AI (color) and the original results from Figure 4 (grey). The inset in panel A and panel E show the variation in the density of Recovered for the two configurations: Equal transmission probability has $\mu = 1.0$; reduced II and MI transmission have $\mu = 0.5$. The different rate of recovery is the complementary effect of the accelerated dynamics.

Figure 7: Equal probability of transmission for MI and AI (30% Scenario).

4.3.2 Transmission from Contained Cases

A second variant was studied by considering the possibility of infection transmission also for individuals in state C. In our model, this means that a person in state S could turns into II also because of peers in the contact network in state C. This variant is a broad approximation of the spreading of infection in isolated conditions like in hospitals or quarantined houses. Such a scenario represents one of the most critical aspects for epidemic management and its modeling has been the subject of specific studies [18, 24]. Here, we want to qualitatively study how a change in this assumption would affect the overall dynamics. The parameter setting in this case has been particularly hypothetical due to the lack of reliable figures for the COVID-19 epidemic. Anecdotally, it appears as non-negligible with respect to the total [21], therefore we have tentatively set the reduction factor $\mu = 0.1$, meaning that the probability of spreading the infection from state C is one tenth of that from state AI. Results are presented in Figure 8 and they reveal a limited impact on the overall dynamics. An increase in the number of infected cases could be observed, distributed accordingly to the proportions between compartments. Therefore, the case of infection spreading in contained facilities could be certainly critical, but probably not because of a particular sensitivity of the natural dynamics. This further emphasizes the current lack of data and points to the need of a specific, detailed treatment of this case.

4.4 Sensitivity of Parameter Estimates

Several tests on model sensitivity with respect to parameter estimates have been run. Specifically, estimates regarding time periods, with associated probability distribution, have been considered. These parameters represent how long an individual remains in state II, AI, and MI before moving to the next state. These are typical epidemiological estimates that we have taken from the current COVID-19 research, comparing different samples and regions. The time frames from the onset of acute symptoms (AI) to containment (C), and form the onset of mild symptoms (MI) to spontaneous recovery (R) seem well-established by epidemiologists with small variability between different studies. For this reason, we concentrate the sensitivity analysis on the infectious period while incubating the disease. For that parameter, which in our model represents the infectious time frame while in incubating state, evidence is still limited. According to the findings of [26], the assumption of [27], and the model fitting real data of Figure 3, we have estimated that parameter with a gamma distribution bounded between 2 and 14 time steps with mean equals to 8 (shape factor equal to 3) ($gamma(T_{II})$ in Figure 2). In particular, we tested both the case of shorter time frames (i.e. period between 2 and 5 time steps, with means equals to 3) and the case of same period but smaller mean (i.e. period between 2 and 14 time steps, with mean equals to 3). Figure 9 shows the result for the case of time frame in [2,5] time steps and mean=3, compared with the original setting; the 30% Scenario configuration is the base line. As expected, a reduction

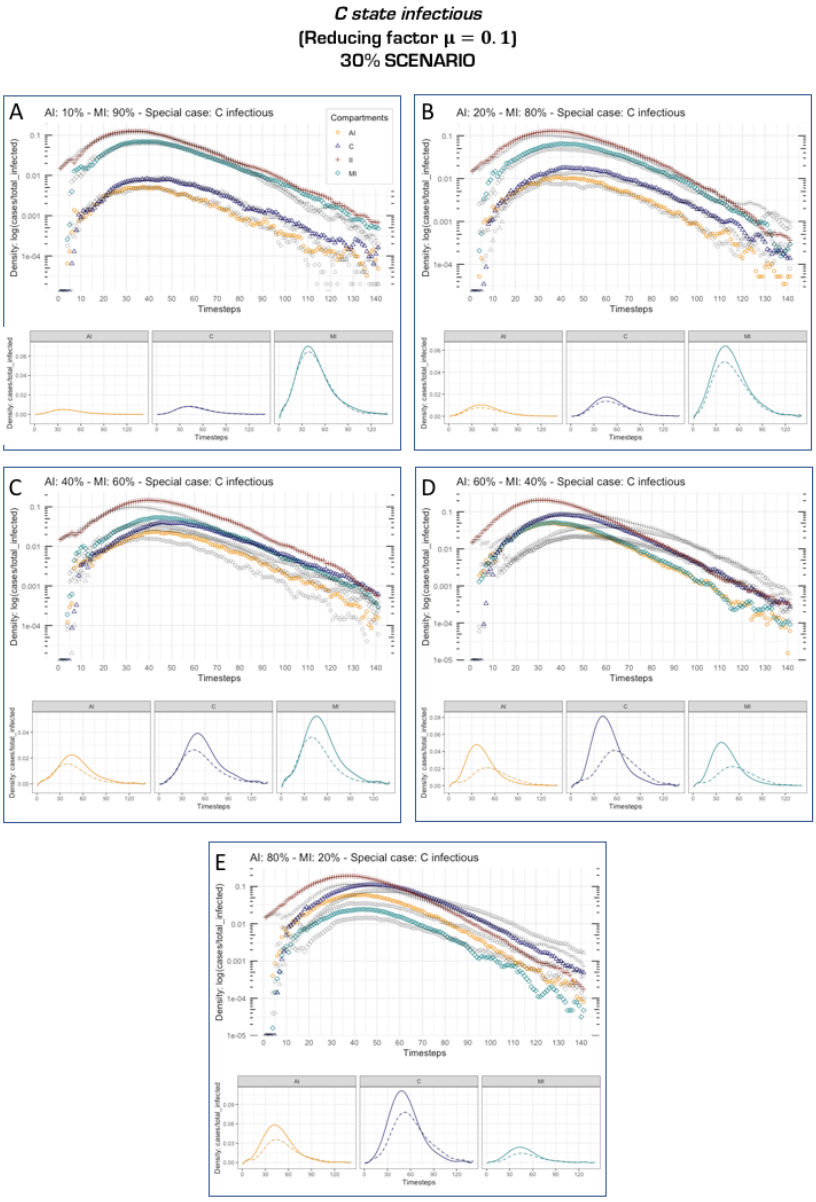

For an individual in state S, the probability to be infected by a peer in state C is assumed to be 1/10 of the probability to be infected by a peer in state AI. *Panels Top*: Comparison of results with a probability of transmission of state C (color) or no transmission (grey). *Panels Bottom*: Dashed line: no trans. from C; Solid line: trans. from C.

Figure 8: Probability of transmission of state C (Reduction factor $\mu = 1.0$).

in absolute values of infected cases could be observed, deriving from the fact that, with a shorter time frame and smaller mean, an individual in II has fewer chances to infect S peers. What was unanticipated is the evident acceleration of the dynamics, whose extent is not linearly dependent on the reduction of the number of infected. The result has been replicated with different configurations and it mostly depends on the mean. This case is interesting because it represents another exhibit of the accelerated dynamic effect discussed before. For a dynamic of this kind, the risk posed by the MI compartment at the end of the epidemics naturally disappears and the C compartment is always a safe proxy for evaluating the reduction of the unknown MI cases. However, this type of dynamics, we have verified to fail to fit the data of the COVID-19 and, for this reason, we deemed it as not useful for the risk analysis.

4.5 Mitigating Strategies

Finally, we analyze possible strategies for managing the final phase risk. As already anticipated in the presentation of previous tests, a risks driven by the uncertain MI class arise when its dynamics outlives those of the other observable classes, namely AI and C. On the contrary, risks decrease when observable classes have a dynamic close to that of MI and therefore could be considered a good proxy. As we have seen from results, in practice it is always the C class, not the AI, to be the candidate for approximating the behavior of MI. As a consequence, a mitigation strategy, with respect to the natural dynamics studied in this work and for configurations with a large majority of MI with respect to AI, could be to force the dynamics of the C class to get sufficiently close to that of the MI class. More specifically, this means to act on the dynamic model in order to push a sufficiently large proportion of MI to move into the C class, instead of naturally terminating in R. In practical terms, this means being able to identify MI cases with test or screening campaigns and restrict them. Figure 10 shows the results of these tests. Panel A is the case with no MI moving to C, and could be confronted with panels B-D with an increasing proportion of MI moving to C. As expected, the effect is that MI and C behaviors tend to come closer, with MI decreasing and C increasing. It could be observed that it exists a certain proportion of MI ending up in C that makes the two curves almost completely overlapping in the final phase of the epidemic wave (see Figure 10 panel C), while for larger proportions, the C curve exceeds the MI (Figure 10 panel D). As we have already seen, the number of infected AI appears to be a poor proxy for evaluating MI in all conditions with MI greater than AI. Alternatively, it could be interesting to analyze under what conditions the class C, which we assume to be observable from official reports, could approximate the unknown MI. From Figure 10 panel E, the relevant information is whether the C/MI rate falls close to, above, or below the intercept at $y = 1$, respectively meaning that:

- $C/MI \approx 1$: the behaviors of C and MI are alike, therefore C could possibly be an acceptable approximation of MI;

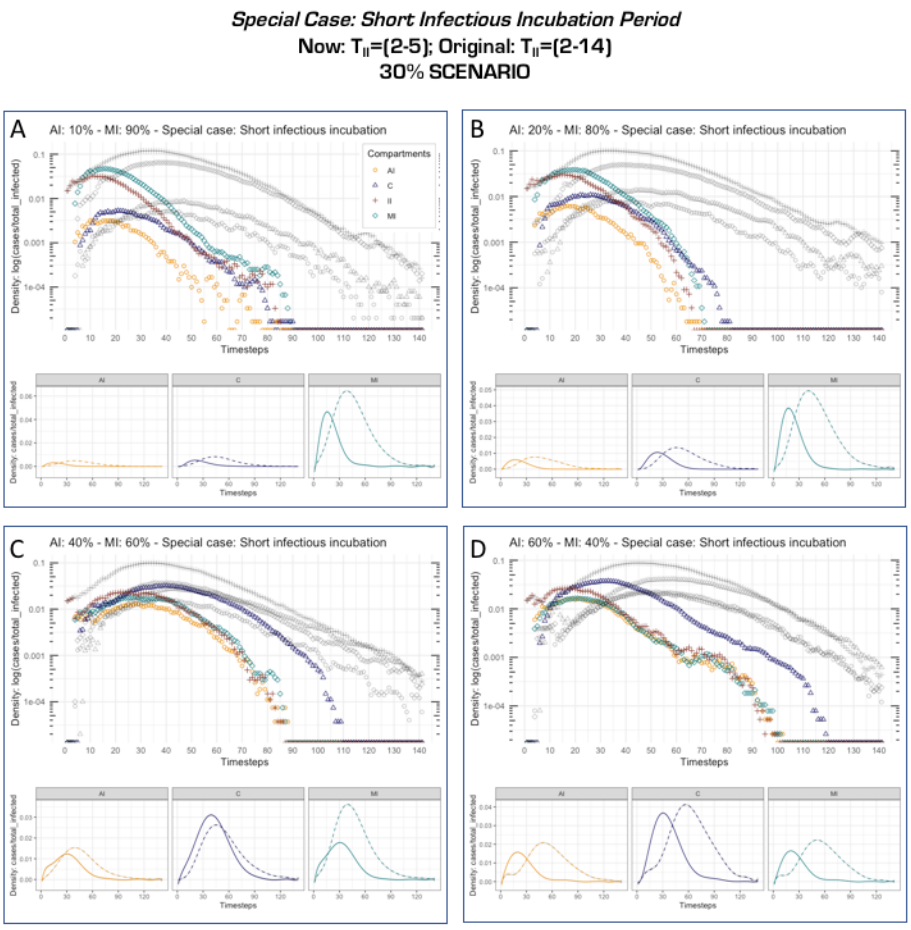

Panels Top: Comparison of results with a short T_{II} and reduced mean (color, $T_{II} = (2, 5)$, mean=3) with original configuration (grey, $T_{II} = (2, 14)$, mean=8). *Panels Bottom*: Solid line: Short time period, reduced mean; Dashed line: Original configuration.

Figure 9: Results for short infectious incubation time period and smaller mean.

- $C/MI >> 1$: the C class will extinguish after the MI has extinguished, then C is a safe predictor of MI;
- $C/MI << 1$: when the C extinguishes, the MI class has still (possibly numerous) active cases, therefore C is not a safe predictor of MI.

Model simulations of the 30% Scenario show that C is a good proxy for MI when a relevant proportion of MI is diagnosed and move to C (MI_to_C = 50% and 80%). This indicates that it is possible to effectively define a strategy to curb the risk posed by unknown MI cases. The possibility exists to consider C as the observable compartment suitable for risk management planning, and then wait for the recovery time needed to extinguish compartment C. On the other hand, these results show that it is not necessarily a safe choice to consider C as a good approximation of MI. It depends on the specific epidemic behavior (attack rate), it may depend on how reliable is the estimate of the proportion of MI to AI, and it could depend on the effectiveness of the identification of MI cases. This last possibility is probably the more practical to realize through testing and screening campaigns. Similar analyses performed on the 10% and 50% scenarios have confirmed these conclusions.

5 Discussion

Returning to the initial research question (i.e., under which conditions, as a result of the natural evolution of the model, in the final phase of an epidemic wave the undetected infectious cases could represent a high risk situation?), we have presented some tentative answers that, on the one side, could help to inform public health authorities in their decision process, and on the other, have perhaps considered the problem from a different angle with respect to epidemiological studies. In particular, epidemiological models of COVID-19, so far, have almost always been defined to produce forecasts of the epidemic on different time frames. They are typically very rich in compartments and modeled features, both for possible transmission paths and for mitigation strategies. The richness of a prediction model, however, sometimes falls short in revealing more general characteristics of a dynamic network. That is one aspect for which our work offers a contribution: To restrict the scope of the analysis on the final phase of the epidemic wave and propose a systemic analysis based on some peculiar features that have been suggested for COVID-19 epidemic.

The scenarios and variations that we have discussed show that the uncertainty that still persists on the actual epidemic dynamics may produce unfavorable conditions for pragmatic decisions by public health authorities and this is a risk that should be carefully considered. On the other hand, we have also seen that the uncertainty is not unmanageable. Instead, if efforts are directed to obtain solid estimates of some properties, such as the proportion of MI over the population of infected, or the rate of identification and containment of MI, both descriptive and prediction models could greatly improve.

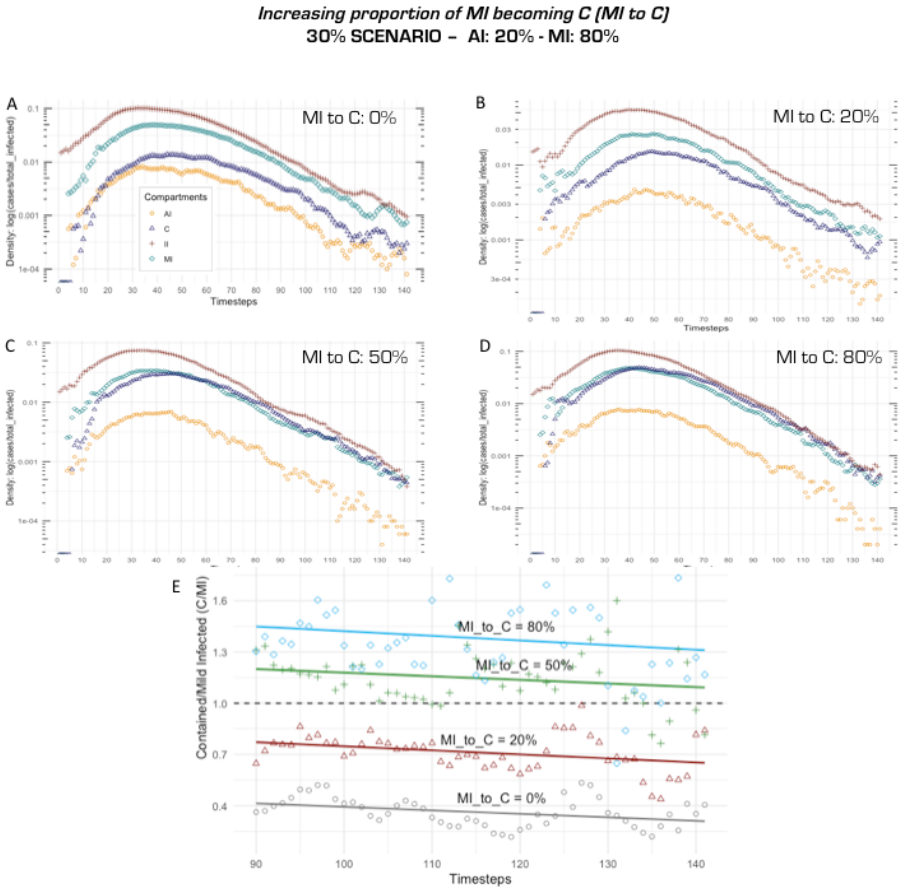

Panel A: System dynamics with no MI ending up into C; *Panels B, C, and D*: Increasing proportions of MI becoming C (i.e., MI_to_C = 20%, 50%, and 80%). The horizontal dotted line at intercept 1.0 on the y-axis represent the ideal threshold for C dynamics to behave as MI. In proximity of this threshold, we could consider that C could be a suitable proxy for MI. Below this threshold, it means that C cases (observable, by definition) tend to lag behind MI cases (not observable, by definition), thus the risk situation may arise. Instead, above the threshold (e.g., MI_to_C = 50% or 80%), it means that MI dynamics tends to lag behind C, which represents a structurally safe condition for managing risks in the final phase of the epidemic.

Figure 10: Additional results of C/MI (similarity of C with respect to MI) for increasing proportions of MI ending up in C (MI_to_C) for configuration AI:MI = 20:80 under the 30% Scenario.

A second important aspect that informed our work was the risk analysis approach. The goal in this case was to identify structural conditions that make a decision in a certain situation (i.e., the final phase of the epidemic wave with the expected social pressure for lifting restrictions) better off or worse off with respect to important uncertain factors and unknowns. To this aim, as we have discussed, factors influencing the epidemic dynamics could be evaluated in different ways. [12] observed that the effects of lifting early the lockdown are better manageable if the proportion of asymptomatic is large, because they will not clog hospital capacity. A possible ambiguity that could then arise from similar prediction approaches is to consider asymptomatic cases as highly relevant for the initial growth phase and instead less critical for the decreasing one. In our analysis, instead, we have seen that the interplay between the infectious classes MI, AI, and C could most often produce the conditions for a high risk in the final phase when the MI class is the large majority. Considering both type of consequences, derived from rich epidemiological models and from systemic ones, and finding the best trade-off between them in public health decisions is one of the most difficult problem that public health authorities have to tackle with.

6 Conclusions

In this paper, we focused on a systemic analysis of some features of the current COVID-10 pandemic. In particular, we studied the natural dynamics possibly emerging in the final phase of the epidemic wave, discussing the conditions that produce risk scenarios for public health authorities in their decision to lift isolation measures. The unfortunate prospect could be made possible by the combination of two factors: the unusual large number of undetected (asymptomatic or mildly ill) cases [3], and, secondly, how people and public health authorities will behave at the end of the epidemic wave, when the perceived risk would rapidly decline and a mounting pressure to remove social distancing measures and reopen circulation in public places will be inevitable. In that situation, the risk is that susceptible individuals and covert infected ones could mix again in an uncontrolled way, and for public health authorities and governments it would be arduous to maintain increasingly unpopular social distancing measures.

We studied several scenarios and special cases, showing that two general properties emerges: that the risk scenario due to the unknown rate of undetected cases might arise when those cases largely outnumber detected and contained cases; and that it is possible, under certain condition, to safely approximate the dynamics of the unknown class with that of an observable one like the contained cases. Furthermore, we analyzed some relevant implications of an accelerated epidemic dynamics with respect to a slower one. However, the theoretical perspective of the natural system dynamics should be complemented with a practical, operational analysis of the consequences.

With our findings, we aim at highlighting the benefits that could possibly come from epidemic models and scenario simulations to public health authorities

facing difficult decisions of crisis management in the last phase of the epidemic wave. One critical issue that the COVID-19 epidemic seems to reveal is the uncertainty regarding its actual characteristics, apparently baffling even experienced epidemiologists. It is this uncertainty level, in our opinion, that calls for risk analysis to be developed together with traditional epidemiology analysis.

References

[1] Joel Achenbach, Wan William, and H. Sun Lena. Coronavirus forecasts are grim: It's going to get worse. *The Washington Post*, 2020.

[2] Cleo Anastassopoulou, Lucia Russo, Athanasios Tsakris, and Constantinos Siettos. Data-based analysis, modelling and forecasting of the COVID-19 outbreak. *PloS one*, 15(3):e0230405, 2020.

[3] Roy M Anderson, Christophe Fraser, Azra C Ghani, Christl A Donnelly, Steven Riley, Neil M Ferguson, Gabriel M Leung, Tai H Lam, and Anthony J Hedley. Epidemiology, transmission dynamics and control of SARS: the 2002–2003 epidemic. *Philosophical Transactions of the Royal Society of London. Series B: Biological Sciences*, 359(1447):1091–1105, 2004.

[4] Roy M Anderson, Hans Heesterbeek, Don Klinkenberg, and T Déirdre Hollingsworth. How will country-based mitigation measures influence the course of the covid-19 epidemic? *The Lancet*, 395(10228):931–934, 2020.

[5] Julien Arino, Fred Brauer, Pauline van den Driessche, James Watmough, and Jianhong Wu. Simple models for containment of a pandemic. *Journal of the Royal Society Interface*, 3(8):453–457, 2006.

[6] Sarah Boseley. Coronavirus 'could infect 60% of global population if unchecked'. *The Guardian*, 2020.

[7] Fred Brauer. Some simple epidemic models. *Mathematical Biosciences & Engineering*, 3(1):1, 2006.

[8] Fred Brauer. Compartmental models in epidemiology. In *Mathematical epidemiology*, pages 19–79. Springer, 2008.

[9] Elizabeth Bruch and Jon Atwell. Agent-based models in empirical social research. *Sociological methods & research*, 44(2):186–221, 2015.

[10] Andrew D Cliff and Peter Haggett. A swash–backwash model of the single epidemic wave. *Journal of geographical systems*, 8(3):227–252, 2006.

[11] Mark DM Davis, Niamh Stephenson, Davina Lohm, Emily Waller, and Paul Flowers. Beyond resistance: social factors in the general public response to pandemic influenza. *BMC public health*, 15(1):436, 2015.

[12] Laura Di Domenico, Giulia Pullano, Chiara E. Sabbatini, Pierre-Yves Boëlle, and Vittoria Colizza. Expected impact of lockdown in Île-de-france and possible exit strategies. Report 9, EPIcx lab, 2020.

[13] Dipartimento della Protezione Civile. Dati COVID-19 Italia. Presidenza del Consiglio dei Ministri, 2020.

[14] Stephen Eubank, Hasan Guclu, VS Anil Kumar, Madhav V Marathe, Aravind Srinivasan, Zoltan Toroczkai, and Nan Wang. Modelling disease outbreaks in realistic urban social networks. *Nature*, 429(6988):180–184, 2004.

[15] Neil M Ferguson, Derek AT Cummings, Simon Cauchemez, Christophe Fraser, Steven Riley, Aronrag Meeyai, Sopon Iamsirithaworn, and Donald S Burke. Strategies for containing an emerging influenza pandemic in Southeast Asia. *Nature*, 437(7056):209–214, 2005.

[16] Seth Flaxman, Swapnil Mishra, Axel Gandy, H Unwin, H Coupland, T Mellan, H Zhu, T Berah, J Eaton, P Perez Guzman, et al. Report 13: Estimating the number of infections and the impact of non-pharmaceutical interventions on COVID-19 in 11 European countries. 2020.

[17] Tapiwa Ganyani, Cecile Kremer, Dongxuan Chen, Andrea Torneri, Christel Faes, Jacco Wallinga, and Niel Hens. Estimating the generation interval for covid-19 based on symptom onset data. *medRxiv*, 2020.

[18] Denise Li-Meng Goh, Bee Wah Lee, Kee Seng Chia, Bee Hoon Heng, Mark Chen, Stefan Ma, and Chorh Chuan Tan. Secondary household transmission of SARS, Singapore. *Emerging infectious diseases*, 10(2):232, 2004.

[19] Abba B Gumel, Shigui Ruan, Troy Day, James Watmough, Fred Brauer, P Van den Driessche, Dave Gabrielson, Chris Bowman, Murray E Alexander, Sten Ardal, et al. Modelling strategies for controlling SARS outbreaks. *Proceedings of the Royal Society of London. Series B: Biological Sciences*, 271(1554):2223–2232, 2004.

[20] Petter Holme and Jari Saramäki. Temporal networks. *Physics reports*, 519(3):97–125, 2012.

[21] International Council of Nurses. High proportion of healthcare workers with COVID-19 in Italy is a stark warning to the world: protecting nurses and their colleagues must be the number one priority. 2020.

[22] Yichuan Jiang and JC Jiang. Diffusion in social networks: A multiagent perspective. *IEEE Transactions on Systems, Man, and Cybernetics: Systems*, 45(2):198–213, 2014.

[23] Matt J Keeling and Ken TD Eames. Networks and epidemic models. *Journal of the Royal Society Interface*, 2(4):295–307, 2005.

[24] Lincoln LH Lau, Hiroshi Nishiura, Dennis KM Heath Kelly, Gabriel M Leung, and Benjamin J Cowling. Household transmission of 2009 pandemic influenza A (H1N1): a systematic review and meta-analysis. *Epidemiology (Cambridge, Mass.)*, 23(4):531, 2012.

[25] Michael Le Page and Debora Mackenzie. Could the new coronavirus really kill 50 million people worldwide? *New Scientist*, 2020.

[26] Peng Li, Ji-Bo Fu, Ke-Feng Li, Yan Chen, Hong-Ling Wang, Lei-Jie Liu, Jie-Nan Liu, Yong-Li Zhang, She-Lan Liu, An Tang, et al. Transmission of COVID-19 in the terminal stage of incubation period: a familial cluster. *International Journal of Infectious Diseases*, 2020.

[27] Ruiyun Li, Sen Pei, Bin Chen, Yimeng Song, Tao Zhang, Wan Yang, and Jeffrey Shaman. Substantial undocumented infection facilitates the rapid dissemination of novel coronavirus (SARS-CoV2). *Science*, 2020.

[28] Ira M Longini, M Elizabeth Halloran, Azhar Nizam, and Yang Yang. Containing pandemic influenza with antiviral agents. *American journal of epidemiology*, 159(7):623–633, 2004.

[29] Ira M Longini, Azhar Nizam, Shufu Xu, Kumnuan Ungchusak, Wanna Hanshaoworakul, Derek AT Cummings, and M Elizabeth Halloran. Containing pandemic influenza at the source. *Science*, 309(5737):1083–1087, 2005.

[30] Emanuele Massaro, Alexander Ganin, Nicola Perra, Igor Linkov, and Alessandro Vespignani. Resilience management during large-scale epidemic outbreaks. *Scientific reports*, 8(1):1–9, 2018.

[31] Kenji Mizumoto, Katsushi Kagaya, Alexander Zarebski, and Gerardo Chowell. Estimating the asymptomatic proportion of coronavirus disease 2019 (COVID-19) cases on board the Diamond Princess cruise ship, Yokohama, Japan, 2020. *Eurosurveillance*, 25(10):2000180, 2020.

[32] Romualdo Pastor-Satorras, Claudio Castellano, Piet Van Mieghem, and Alessandro Vespignani. Epidemic processes in complex networks. *Reviews of modern physics*, 87(3):925, 2015.

[33] Fotios Petropoulos and Spyros Makridakis. Forecasting the novel coronavirus COVID-19. *Plos one*, 15(3):e0231236, 2020.

[34] Kiesha Prem, Yang Liu, Timothy W Russell, Adam J Kucharski, Rosalind M Eggo, Nicholas Davies, Stefan Flasche, Samuel Clifford, Carl AB Pearson, James D Munday, et al. The effect of control strategies to reduce social mixing on outcomes of the COVID-19 epidemic in Wuhan, China: a modelling study. *The Lancet Public Health*, 2020.

[35] Jane Qiu. Covert coronavirus infections could be seeding new outbreaks. *Nature*, 2020.

[36] Marcel Salathe, Linus Bengtsson, Todd J Bodnar, Devon D Brewer, John S Brownstein, Caroline Buckee, Ellsworth M Campbell, Ciro Cattuto, Shashank Khandelwal, Patricia L Mabry, et al. Digital epidemiology. *PLoS computational biology*, 8(7), 2012.

[37] Juliette Stehlé, Nicolas Voirin, Alain Barrat, Ciro Cattuto, Vittoria Colizza, Lorenzo Isella, Corinne Régis, Jean-François Pinton, Nagham Khanafer, Wouter Van den Broeck, et al. Simulation of an SEIR infectious disease model on the dynamic contact network of conference attendees. *BMC medicine*, 9(1):87, 2011.

[38] The Humanitarian Data Exchange. Coronavirus COVID-19 Cases Data for China and the Rest of the World, 2020.

[39] The New York Times. Coronavirus (Covid-19) Data in the United States, 2020.

[40] Lirong Zou, Feng Ruan, Mingxing Huang, Lijun Liang, Huitao Huang, Zhongsi Hong, Jianxiang Yu, Min Kang, Yingchao Song, Jinyu Xia, et al. SARS-CoV-2 viral load in upper respiratory specimens of infected patients. *New England Journal of Medicine*, 382(12):1177–1179, 2020.